Vaccine 34 (2016) 5251–5261

Contents lists available at ScienceDirect

Vaccine

journal homepage: www.elsevier.com/locate/vaccine

The primary immune response to *Vaccinia virus* vaccination includes cells with a distinct cytotoxic effector CD4 T-cell phenotype

C. Mee Ling Munier [a,*], David van Bockel [a], Michelle Bailey [a], Susanna Ip [a], Yin Xu [a], Sheilajen Alcantara [b], Sue Min Liu [d], Gareth Denyer [e], Warren Kaplan [d], PHIIDO Study group, Kazuo Suzuki [a,c], Nathan Croft [h], Anthony Purcell [h], David Tscharke [i], David A. Cooper [a,c], Stephen J. Kent [b,f,g], John J. Zaunders [a,c,1], Anthony D. Kelleher [a,c,1]

[a] *The Kirby Institute for infection and immunity in society, UNSW Australia, Sydney, NSW, Australia*
[b] *Department of Microbiology and Immunology, Peter Doherty Institute, University of Melbourne, Melbourne, VIC, Australia*
[c] *St Vincent's Hospital, Sydney, NSW, Australia*
[d] *The Garvan Institute, Sydney, NSW, Australia*
[e] *School of Molecular Bioscience, Faculty of Science, The University of Sydney, NSW, Australia*
[f] *Melbourne Sexual Health Centre and Department of Infectious Diseases, Alfred Health, Central Clinical School, Monash University Melbourne, VIC, Australia*
[g] *ARC Centre of Excellence in Convergent Bio-Nano Science and Technology, University of Melbourne, Parkville, VIC, Australia*
[h] *Infection and Immunity Program, Department of Biochemistry and Molecular Biology, Biomedicine Discovery Institute, Monash University, Clayton, VIC, Australia*
[i] *John Curtin School of Medical Research, The Australian National University, Canberra, ACT, Australia*

ARTICLE INFO

Article history:
Received 23 February 2016
Received in revised form 9 August 2016
Accepted 6 September 2016
Available online 14 September 2016

Keywords:
Vaccinia
Granzyme K
CD4
CD8
Microarray
HIV
Cytotoxic T-cells

ABSTRACT

Background: Smallpox was eradicated by a global program of inoculation with *Vaccinia virus* (VV). Robust VV-specific CD4 T-cell responses during primary infection are likely essential to controlling VV replication. Although there is increasing interest in cytolytic CD4 T-cells across many viral infections, the importance of these cells during acute VV infection is unclear.

Methods: We undertook a detailed functional and genetic characterization of CD4 T-cells during acute VV-infection of humans. VV-specific T-cells were identified by up-regulation of activation markers directly *ex vivo* and through cytokine and co-stimulatory molecule expression. At day-13-post primary inoculation with VV, CD38highCD45RO+ CD4 T-cells were purified by cell sorting, RNA isolated and analysed by microarray. Differential expression of up-regulated genes in activated CD4 T-cells was confirmed at the mRNA and protein levels. We compared analyses of VV-specific CD4 T-cells to studies on 12 subjects with primary HIV infection (PHI). VV-specific T-cells lines were established from PBMCs collected post vaccination and checked for cytotoxicity potential.

Results: A median 11.9% CD4 T-cells were CD38highCD45RO+ at day-13 post-VV inoculation, compared to 3.0% prior and 10.4% during PHI. Activated CD4 T-cells had an up-regulation of genes related to cytolytic function, including granzymes K and A, perforin, granulysin, TIA-1, and Rab27a. No difference was seen between CD4 T-cell expression of perforin or TIA-1 to VV and PHI, however granzyme k was more dominant in the VV response. At 25:1 effector to target ratio, two VV-specific T-cell lines exhibited 62% and 30% cytotoxicity respectively and CD107a degranulation.

Conclusions: We show for the first time that CD4 CTL are prominent in the early response to VV. Understanding the role of CD4 CTL in the generation of an effective anti-viral memory may help develop more effective vaccines for diseases such as HIV.

1. Introduction

CD4 T-cells play a crucial role in a functioning immune system and are critical for durable anti-viral immunity. They assist B cells to produce neutralizing antibodies and augment and maintain virus-specific CD8 T-cell responses. CD4 T-cells with cytotoxic characteristics have been increasingly described *ex vivo* and have

* Corresponding author at: Immunovirology and Pathogenesis Program, The Kirby Institute, UNSW, Australia, Wallace Wurth Building, Sydney, NSW 2052, Australia.
E-mail address: cmunier@kirby.unsw.edu.au (C. Mee Ling Munier).
[1] These authors contributed equally to this work.

http://dx.doi.org/10.1016/j.vaccine.2016.09.009
0264-410X/

been linked to control a number of viral infections affecting humans, including HIV-1 [1–4], CMV [5,6], EBV [7] and viral hepatitis [8]. Cytotoxic CD4 T-cells have also been detected in individuals vaccinated against poliovirus [9] and in the RV144 HIV vaccine study [10]. In macaques, simian immunodeficiency virus (SIV)-specific CD4 T-cells were shown to have direct effector function with the ability to eliminate SIV-infected macrophages *ex vivo* [11].

The role of cytotoxic CD4 T-cells during a robust experimental infection of humans such as *Vaccinia virus* (VV) has not been studied. VV provides an attractive model to study human anti-viral T-cell responses as: (i) this live virus vaccination results in acute infection that is cleared leading to life-long immunity [12]; (ii) the effectiveness of immunity has been demonstrated by global eradication of smallpox; (iii) un-controlled antigenic re-exposure is unlikely, so measurement of memory most likely reflects cells generated by vaccination; (iv) exact date and strain of inoculation with VV is known, unlike most primary HIV-1, EBV and CMV infections, hence it is possible to undertake scheduled prospective longitudinal studies to dissect early stages of the immune response.

The peak of the primary VV-specific CD4 T-cell response occurs ~2 weeks after inoculation, with a sharp increase in highly activated cells (CD4+CD38+++) that produce IFN-γ, have high proliferative and apoptotic rates and approximately half express CTLA-4 [13]. A similar pattern of early-activated effector CD4 T-cells in primary HIV-1 infection (PHI) has been observed, however, CD127 expression and IL-2 is lower and CTLA-4 higher than in VV-specific cells [2,14]. It is likely such differences in these two primary immune responses reflect differences in effectiveness of subsequent memory responses in these two infections, but the determinants of these differences are not understood.

In the current study, we sought to further understand differences in the primary immune response to VV and primary immune response to HIV-1 by comparing immunophenotype of T-cells from these two groups. Analysis of microarray data generated from sorted human CD4 T-cells at day-13 post-VV vaccination revealed that activated CD4 T-cells have a prominent cytotoxic T lymphocyte (CTL) profile with up-regulation of CTL associated genes including granzyme (Gzm) K and A.

2. Materials and methods

2.1. Subjects

Individuals receiving primary VV-immunisation (Dryvax vaccine, Wyeth Laboratories, Marietta, PA, USA) for occupational requirements were recruited. Blood drawn prior to vaccination (baseline), at day-13 and 12-months post-vaccination (Supplementary Fig. 1). Cryopreserved PBMCs from 12 individuals with acute PHI enrolled in the Primary HIV Infection Identification, Data collection and Observation (PHIIDO) cohort were used.

VV studies were approved by Australian Red Cross Blood Service Human Research Ethics Committee (HREC), St Vincent's Hospital Sydney HREC (HREC/10/SVH/130) and University of Melbourne Health Sciences Human Ethics Sub-Committee (Ethics ID: 1035129). PHIIDO cohort studies were approved by St Vincent's Hospital Sydney HREC (HREC/08/SVH/180). All participants gave informed written consent.

2.2. Reagents

The monoclonal antibodies used: CD3PerCP-Cy5.5, CD4AlexaFluor-700, CD4-PE-Cy7, CD4BV605, CD8APC-Cy7, CD8-FITC, CD25APC, CD38-PE, CD38PE-Cy7, CD45RA-APC, CD69-PE, CD107a-APC, CD134 (OX40)-PE, Beta-7-APC, Bcl-2-PE, CCR5-PE, CXCR3-PE-CF594, IFN-γ-APC, IFN-γ-FITC, IL-2-PE, Ki-67-FITC, TNF-α-PE-Cy7 (Becton Dickinson (BD), San Jose, CA, USA); CD4-energy coupled dye (ECD), CD45RO-ECD (Beckman Coulter, Hialeah, FL, USA); GzmK-FITC (Santa Cruz Biotechnology, Santa Cruz, CA, USA); CCR6-BV421, CD127-BV421, GzmA-Pacific Blue, Perforin-PE (BioLegend, San Diego, CA, USA); GzmB-APC, LIVE/DEAD™ Fixable Near-IR, Zenon® Pacific Blue™ Mouse IgG_1 labelling kit (Molecular Probes, Eugene, OR, USA); CD62L-eFluor780, Eomes-APC, T-bet-PE (eBioscience); TIA-1-unconjugated (Immunotech), according to manufacturers' directions.

2.3. Immunophenotyping and antigen-specific T-cell assays

Na-Hep anti-coagulated blood was used for immunophenotyping, intracellular cytokine staining assay (ICS) and CD25/OX40 assay as previously described [13,15,16]. For ICS and CD25/OX40 assays, blood was stimulated with: (i) no antigen (negative control); (ii) Staphylococcal enterotoxin B (SEB; positive control; final concentration 1 μg/mL; Sigma, St Louis, MO, USA); (iii) VV lysate and (iv) HeLa cell lysate both at final concentration of 1/250, prepared as described [13]. Gating for ICS in Supplementary Fig. 2a and CD25/OX40 assay in Supplementary Fig. 2b. Samples analysed on 4-Laser LSRII flow-cytometer (BD), data analysed using FlowJo (v9.8.3; TreeStar, Ashland, OR, USA).

2.4. Cell sorting

Cell sorting was performed on 3-Laser FACSAria™ (BD). CD3+CD4+T-cells sorted into: CD45RA+CD38dim (naïve), CD45RAnegCD38+++ (activated effector) and CD45RAnegCD38neg (resting memory) (Supplementary Fig. 3). CD8+CD45RAnegCD38++ also sorted, purity >90–99.8%. Sorted cells lysed in TRIzol® (Invitrogen, Carlsbad, CA, USA), stored at −80 °C.

2.5. RNA extraction from sorted T-cells

For microarray analysis, RNA extraction was performed using modified small-scale method as described [17]. For confirmatory qRT-PCR, RNA was extracted from lysed cells in TRIzol® following manufacturer's protocol.

2.6. Preparation of cRNA and gene-chip hybridizations

Following manufacturer's instructions, Two-Cycle Target Labelling kit (Affymetrix, Inc., Santa Clara, CA, USA) was used to generate cRNA and hybridized to Affymetrix Human Genome U133 Plus 2.0 Arrays (HG-U133 Plus 2.0). Scaling was performed using Microarray Analysis Suite Software 5.0 (Affymetrix).

2.7. Microarray analysis/bioinformatics

Microarray data were normalized, $\log_2$ transformed and analysed with GenePattern (Broad Institute, Cambridge, MA, USA) [18]. Differential gene expression was determined using *LimmaGP* [19] applying multiple testing procedures, producing corrected p-values or q-values for each gene to control for False Discovery Rate (FDR). Q-values <0.05 were considered statistically significant. Comparisons were viewed using *ComparativeMarkerSelection Viewer* and heat maps generated with *HeatMapImage*.

2.8. Conversion of RNA to cDNA for qPCR

RNA was reverse transcribed into cDNA using iScript™ Select cDNA Synthesis Kit (Bio-Rad Laboratories, Hercules, CA, USA) on

an Eppendorf Mastercycler® epgradient S ThermoCycler (Eppendorf, Hamburg, Germany) following kit instructions.

2.9. qRT-PCR for gene expression confirmation

qRT-PCR was performed using primers for GzmB: forward primer, TGGGGGACCCAGAGATTAAAA, reverse primer, TTTCGTCCATAGGAGACAATGC (Geneworks, Hindmarsh, SA, Australia); GzmA: forward primer, GACTCGTGCAATGGAGATTCTGGAA, reverse primer, CCCACGAGGGTCTCCGCATTT; GzmK: forward primer, GCAGCCCACTGCCAATATCGGT, reverse primer, TGGCTCCCCAGCCAGTAACCT (Sigma) and β-actin: forward primer, TCACCCACACTGTGCCCATCTACGA, reverse primer, CAGCGGAACCGCTCATTGCCAATGG [20].

Bio-Rad iQ5 was used for qRT-PCR, using EXPRESS SYBR® GreenER™ qPCR SuperMix Universal (Invitrogen), following manufacturer's instructions. Assays were performed in duplicate with these conditions, 95 °C for 2 min, 50 cycles: 95 °C for 15 s then 60 °C for 1 min, then, melt curve analysis with 81 cycles of 55 °C for 10 s.

2.10. Determination of autologous VV-peptides using mass spectrometry

Mass spectrometry was used to detect VV-epitopes bound to MHC, using immunoaffinity purification and peptide elution [21]. In brief 2×10^9 autologous EBV transformed B-lymphoblastoid cell lines (B-LCL) from PBMC of VV recipients were infected at MOI of 5 with VV-Western Reserve strain (ATCC#VR1354), in serum free DMEM for 30 min. Infected cells were grown in slow rotation for 16 h at 37 °C in DMEM+FCS and L-glutamine. Cells were washed, pelleted and snap-frozen. Frozen cell pellets were ground in a cryogenic mill (Mixer Mill MM 400, Retsch) and lysed in 0.5% IGEPAL, 50 mM Tris pH8.0 and complete protease inhibitor (Roche Molecular Biochemicals). Lysates were cleared by ultracentrifugation and MHC-peptide complexes immunoaffinity purified by Protein A cross-linked to anti-HLA DR mAb (clone L243). Peptides were eluted by addition of 10% acetic acid and purified and fractionated by RP-HPLC separation on ÄKTAmicro™ HPLC system (GE Healthcare) before MS analysis, as described [22].

Peptide fractions were analysed on TripleTOF® 5600+ mass spectrometer (SCIEX) coupled on-line to Eksigent nano LC Ultra 2DPlus combined with a Nanoflex cHiPLC system (SCIEX). Samples were loaded onto trap column (200 μm × 0.5 mm ChromXP C18-CL 3 μm 120 Å) and separated across an analytical column (75 μm × 15 cm ChromXP C18-CL 3 μm 120 Å) under increasing % buffer B (80% acetonitrile in water supplemented with 0.1% formic acid) conditions. Peptides were sequenced using Paragon™ algorithm in ProteinPilot™ (SCIEX) as described [23,24].

Peptides (>75% purity) were purchased from Mimotopes (Clayton, Victoria) and stocks prepared at 10 mg/mL in 100% DMSO.

2.11. Generation of VV-specific T-cell lines

VV specific T-cell lines were generated as described [25]. In brief, PBMC stored at day-13 and 12 months post-vaccination from a VV-vaccinee with HLA-DRB1∗10:01:01 and 15:02:01 were thawed and incubated at 2×10^6 cell/mL in IMDM Glutamax+hAb serum with autologous VV-peptide (final concentration 1 μg/mL). PBMC were stimulated 10 days with peptide, followed by re-stimulation with pre-mixed peptide+irradiated feeder mixture (PBMC+autologous B-LCL (9:1)). Following stimulation with antigen, cells were washed before resting with feeder mixture for 9 days supplemented with 20 U/mL IL-2. Following rest period, cells were cycled through re-stimulation period with VV-peptide for 4 days.

2.12. Cytotoxicity and degranulation assays

The CytoTox96® non-radioactive cytotoxicity assay (Promega, Madison, WI, USA) measures release of lactate dehydrogenase (LDH) following cell lysis, was performed following manufacturer's instructions. Briefly, VV-specific T-cell lines established from 12 months post-VV-vaccination were used as effectors with HLA-matched (HLA-DRB1∗10:01:01 and 15:02:01) and HLA-mismatched (HLA-DRB1∗04:05:01 and 07:01:01G) B-LCL as targets. B-LCL were incubated with 5 μg/mL peptide for 1.5 h at 37 °C in 5% CO_2, seeded into 96 well U-bottom plate at 20,000 cells/well prior to addition of effector cells at different effector:target ratios in triplicate. Following 4 h incubation at 37 °C in 5% CO_2, supernatant was harvested and LDH release measured from target cells. Assay controls included, media alone, LDH spontaneous release from target and effector cells and LDH maximum release from target cells.

The CD107a degranulation assay was performed as described [26]. Briefly, HLA-matched and HLA-mismatched B-LCL were used as antigen presenting cells (APC) and incubated with peptide as above. VV-specific T-cell lines from 13-days (DPL) and 12 months post-vaccination (DPD and DPL) were incubated with B-LCL at different effector:APC ratios with CD107a-APC mAb, diluted BFA and BD GolgiStop for 4 h at 37 °C in 5%CO_2. Following 4 h incubation, cells were permeabilised, stained with mAbs of interest, fixed with PFA and analysed on 4-Laser LSRII flow-cytometer (BD), data analysed using FlowJo (TreeStar).

2.13. Statistical analysis

Unpaired non-parametric Mann-Whitney test and Spearman's correlation were used. P-values <0.05 were considered statistically significant. Prism 6 for Macintosh (GraphPad Software Inc., La Jolla, CA, USA) was used.

3. Results

3.1. Study participant characteristics

VV-vaccine recipients had a median age 24.5 years (range: 20–34 years) and 29% (7/24) were male. PHIIDO cohort individuals had a median age 42 years (range: 26–78 years), were male, untreated and identified within an estimated median 25-days from HIV-1 infection to blood sampling. See Table 1 for PHIIDO participant's clinical characteristics.

3.2. VV-immunization induces high levels of activated and VV-specific CD4 T-cells

By flow cytometry, we measured CD4 T-cells that were activated (CD45RO+CD38+++, Fig. 1a) 13-days following VV-vaccination. A significant (median: 11.9%, Fig. 1b) 4-fold increase in activated CD4 T-cells was found at day-13 compared to baseline (median: 3.02%). 12 months following vaccination, activated CD4 T-cells returned to pre-vaccination levels (median: 3.86%, Fig. 1b). At day-13 post-VV-vaccination, a median 8.6% of CD8 T-cells had an activated phenotype up from 2.4% at baseline and 1.6% at 12 months (Fig. 1b).

CD4 T-cells from individuals studied during PHI had similar levels of activation (median 10.4%, Fig. 1b) to 13-days following VV-vaccination. CD8 T-cells studied during PHI had significantly higher activation (median 53.6%, Fig. 1b) than CD8 responding to VV, despite being measured an estimated median 25-days following HIV-infection.

Table 1
Clinical characteristics of the acute primary HIV+ subjects from the PHIIDO study at diagnosis.

Study ID	Age	Gender	Viral RNA (copies/mL)	p24 antigen (pg/mL)	HIV-1 Antibody (ELISA)	# Western Blot bands	Fiebig stage	Estimated days from infection to blood sampling
PHI 1	52	Male	>750,000	28	Reactive	0	III	25
PHI 2	41	Male	39,726	1720	Reactive	0	III	25
PHI 3	26	Male	>500,000	336	Not reactive	0	II	22
PHI 4	54	Male	47,835	Neg	Reactive	2 (gp160, p24)	V	101
PHI 5	41	Male	186,000	32,340	Reactive	0	III	25
PHI 6	42	Male	15,400	Neg	Not reactive	1 (p24)	IV	31
PHI 7	64	Male	100,000	1236	Reactive	0	III	25
PHI 8	41	Male	57,300	1025	Reactive	0	III	25
PHI 9	41	Male	399,000	3464	Reactive	3 (gp160, p55, p24)	V	101
PHI 10	35	Male	1,035,122	8680	Reactive	0	III	25
PHI 11	50	Male	>100,000	2500	Reactive	1 (p24)	IV	31
PHI 12	78	Male	260,400	Reactive	Reactive	0	III	25

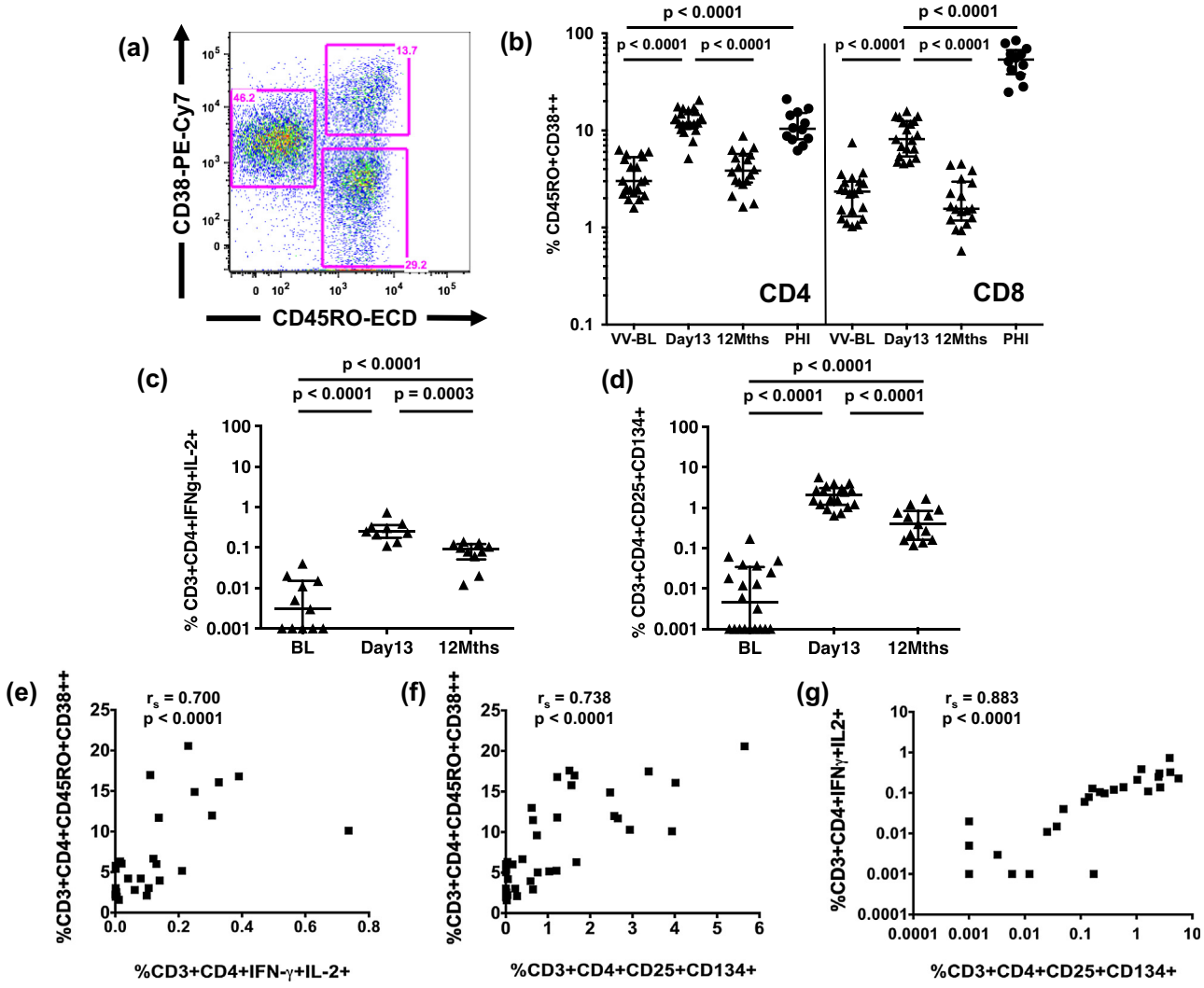

Fig. 1. Immunisation with *Vaccinia virus* induces high levels of activated and vaccinia-specific CD4 T-cells. (a) Representative flow plot of CD3+CD4+ T-cells that are activated (CD45RO+CD38+++), naïve (CD45ROnegCD38dim) and resting (CD45RO+CD38neg) at day-13 post-VV inoculation. Detection of (b) activated CD4 and CD8 T-cells as measured by CD45RO+CD38++ expression (VV: n = 18–20; PHI: n = 12) and VV-specific CD4 T-cells by (c) ICC expression of IFN-γ+IL-2+ (n = 10–11) and (d) co-expression of CD25 +CD134+ from the OX40 assay (n = 13–18) in response to whole VV lysate. Medians and interquartile ranges are shown. Correlation of activated CD4 T-cells with (e) IFN-γ+IL-2+ (n = 28) and (f) CD25+CD134+ VV-specific CD4 T-cells (n = 28), (g) Correlation of the ICS and OX40 antigen-specific CD4 assays (n = 27).

The large increase in activated CD4 T-cells at day-13 post-VV-vaccination was associated with appearance of VV-specific CD4 T-cells detected by ICS (Supplementary Fig. 2a) and CD25/OX40 assays (Supplementary Fig. 2b). At day-13 post-vaccination, a median 0.25% of CD4 T-cells were IFN-γ+IL-2+, significantly higher than baseline (median: 0.003%, Fig. 1c). The median VV-specific CD4 T-cell response in CD25/OX40 assays increased significantly from 0.005% at baseline to 2.1% at day-13

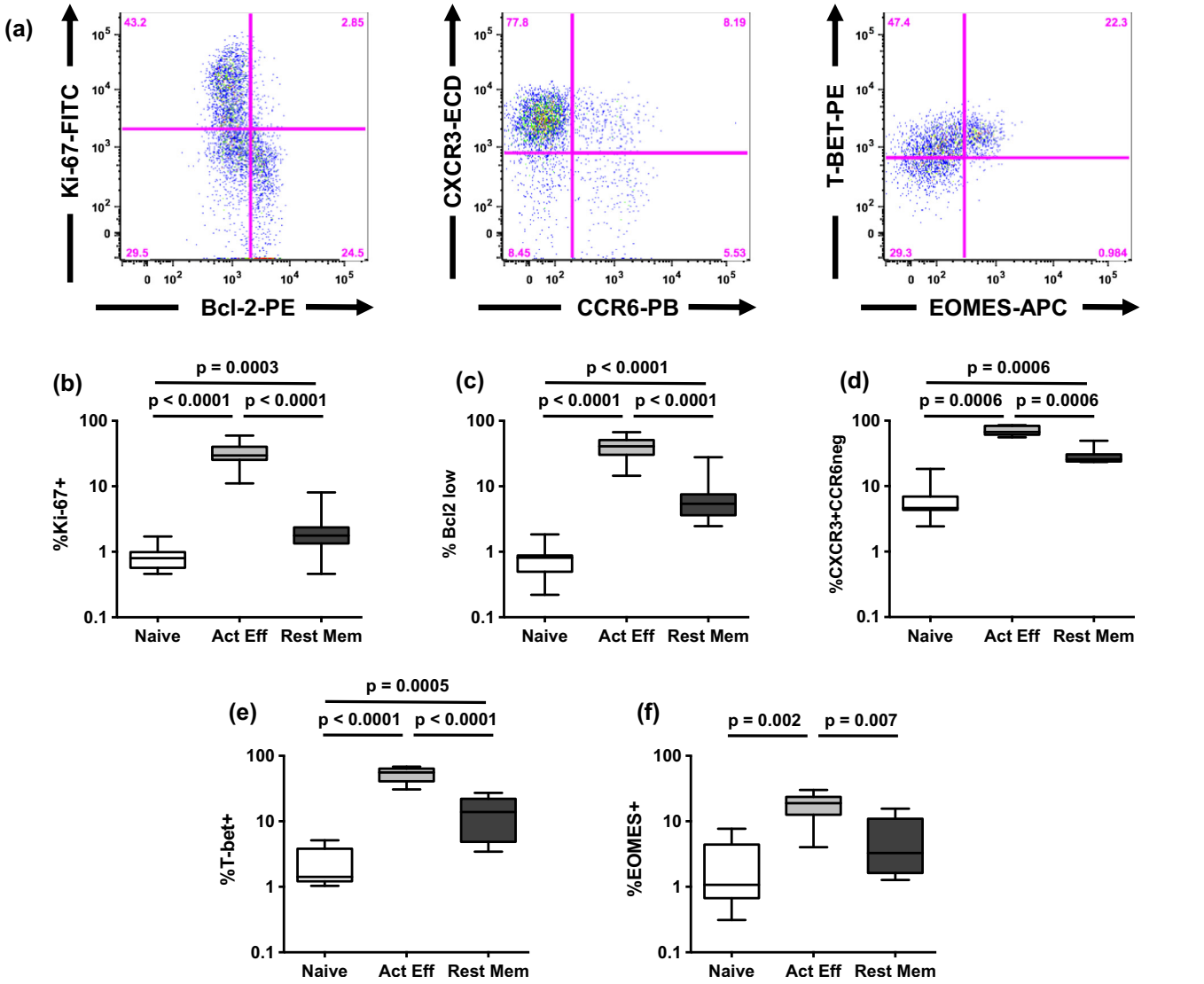

Fig. 2. Phenotype of activated CD4 T-cells following vaccination with *Vaccinia virus*. (a) Representative flow plots of CD3+CD4+ T-cells that are: left: proliferating (Ki-67+) and prone to apoptosis (Bcl-2 low); middle: CXCR3+CCR6neg; right: expressing the transcription factors T-bet and Eomes. Differential expression of (b) Ki-67 (n = 15), (c) Bcl-2low (n = 15), (d) CXCR3 (n = 7), (e) T-bet (n = 9) and (f) Eomes (n = 7) on naïve, activated effector and resting memory CD4 T-cells in response to VV at day-13 following vaccination. The box-and-whisker plots represent the minimum, 25th percentile, median, 75th percentile and maximum values.

(Fig. 1d). At 12-months post-vaccination, VV-specific CD4 T-cells remained detectable by both assays (ICS median: 0.09%, Fig. 1c; CD25/OX40 median: 0.4%, Fig. 1d).

Although levels of activated CD4 T-cells were higher than VV-specific CD4 T-cells measured by ICS and CD25/OX40, it is likely that a significant proportion of activated cells are VV-specific. Antigen-specific assays are likely less sensitive, as some VV-lysate proteins may be poorly expressed or presented, leading to this discrepancy. A significant positive correlation was found between activated CD4 T-cells and VV-specific CD4 T-cells measured by ICS (Fig. 1e) and CD25/OX40 (Fig. 1f). A significant positive correlation was found between the two antigen-specific assays (Fig. 1g).

Ex vivo, activated CD4 T-cells at day-13 post-VV-vaccination were highly proliferative, a median 29.5% expressed Ki-67, representing 10–20 fold-increase over naïve or resting memory cells (Fig. 2a and b). However 40.7% of these cells expressed low Bcl-2, hence were prone to apoptosis and likely destined to be short-term effector cells (Fig. 2a and c). A median 67% of activated CD4 T-cells were CXCR3+CCR6neg (Fig. 2a and d) consistent with a Th1 type response [27,28]. In keeping with the Th1 type response, activated CD4 T-cells had significantly higher expression of T-bet and Eomes, median 55.7% (Fig. 2a and e) and 18.9% (Fig. 2a and f) of cells expressing these transcription factors respectively.

3.3. Microarray of activated effector CD4 T-cells day-13 post-vaccination with VV

Analysis of microarray data with these filters: fold change (FC) >2 and q-value <0.05, revealed 561 genes up-regulated in activated effector CD4 T-cells compared to naïve. Statistically significant up-regulation of genes whose protein products were previously described in activated proliferating T-cells [13], including Ki-67 (FC = 4.7, q = 0.003), CD38 (FC = 2.3, q = 0.01) and CCR5 (FC = 16.3, q = 0.01) was found, serving to validate the arrays (Fig. 3a).

As expected, most of the up-regulated genes were associated with cell cycle, DNA synthesis, DNA repair and proliferation (Fig. 3a) and included ribonucleotide reductase M2 polypeptide

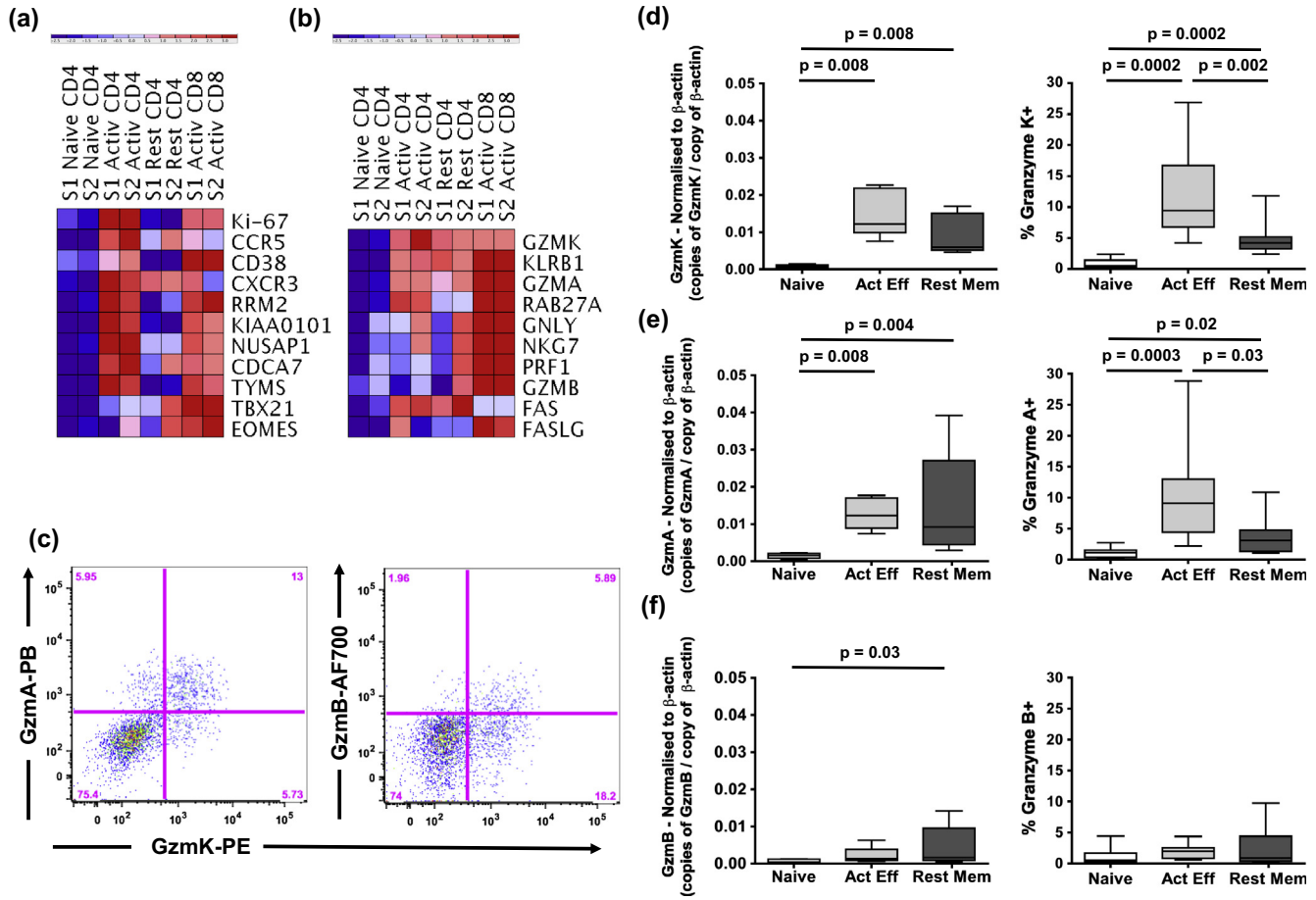

Fig. 3. Detection and confirmation of differential gene expression 13-days following vaccination with *Vaccinia virus*. Microarray analyses were performed on purified T-cells from two individuals. Relative expression of (a) genes associated with cell cycle and proliferation and (b) CTL associated genes, up-regulated in activated effector CD4 T-cells compared to naïve CD4 T-cells at day-13 post-VV vaccination. The columns represent the sorted cell populations of naïve, activated effector and resting memory CD4 T-cells with the last two columns representing the activated CD8 T-cells. There are two columns per cell population due to the two subjects S1 and S2. Blue represents low expression and red represents high expression. (c) Representative flow plots of CD3+CD4+CD38+CD45RO+ T-cells that are expressing GzmA, Gzm B and Gzm K. Confirmation of differential gene expression at the mRNA (n = 5) and protein level (n = 8) for (d) GzmK; (e) GzmA and (f) GzmB. The box-and-whisker plots represent the minimum, 25th percentile, median, 75th percentile and maximum values.

(*RRM2*; FC = 49; q = 0.006); thymidylate synthetase (*TYMS*; FC = 18; q = 0.002); *KIAA0101* (FC = 37; q = 0.002); cell division cycle associated 7 (*CDCA7*; FC = 24; q = 0.007); and nucleolar and spindle associated protein 1 (*NUSAP1;* FC = 25; q = 0.002).

Surprisingly, the array revealed activated CD4 T-cells had a statistically significant up-regulation of genes associated with cytolytic function (Fig. 3b). The gene for GzmK, a trypsin-like serine protease, was most highly expressed (FC = 42; q = 0.008), followed by killer cell lectin-like receptor subfamily B member 1 (*KLRB1*/CD161; FC = 26; q = 0.002), *GzmA* (FC = 14; q = 0.002), *Rab27a* (FC = 8; q = 0.002) and granulysin (*GNLY*; FC = 6; q = 0.43).

Related CTL-associated genes such as the pore forming protein, perforin 1 (*PRF1*; FC = 2.6; q = 0.59) and natural killer cell group 7 sequence (*NKG7*), also known as GMP-17/TIA-1 (FC = 6; q = 0.41) were up-regulated in activated CD4 T-cells (Fig. 3b). However, expression of *GzmB*, a serine protease known to be contained in cytotoxic T-cells was down-regulated 1.5 fold in activated CD4 T-cells (Fig. 3b).

Interestingly, the gene for Fas ligand (*FASL*; FC = 1.5; q = 0.3; Fig. 3b) was slightly up-regulated on activated CD4 T-cells, indicating there was not generalized up-regulation of cytolytic mechanisms. However, the gene for Fas (*FAS*; FC = 7; q = 0.006; Fig. 3b) was up-regulated in activated CD4 T-cells suggesting these cells may be targeted by Fas ligand expressing cells.

3.4. Confirmation of differentially expressed genes at the mRNA and protein levels

GzmK mRNA expression was 17.6 fold-higher in activated CD4 T-cells than in naïve CD4 T-cells (Fig. 3d), differential expression of GzmK protein between these two subsets was of similar magnitude (FC = 17.3, Fig. 3c and d). Similarly, expression of GzmA at the mRNA and protein level was 8 fold-higher in activated CD4 T-cells (Fig. 3c and e). As a comparator gene, GzmB was also analysed, difference in GzmB mRNA or protein expression was found between activated CD4 or naïve CD4 T-cells (Fig. 3c and f), reflecting the microarray results (Fig. 3b).

3.5. CD4 CTL vs CD8 CTL in response to VV and PHI

The cytolytic genes that were up-regulated in activated CD4 T-cells were as expected highly up-regulated in activated CD8 T-cells (Fig. 3b) following VV-vaccination. In contrast to activated CD4 T-cells, *GzmK* expression was 2-fold lower and *GzmB* expression was 100-fold higher in activated CD8 T-cells following VV-vaccination (Fig. 3b). We compared the phenotype of activated CD4 and CD8 T-cells from primary VV-vaccinees and subjects with PHI to determine if differences of selected CTL markers existed in response to the two viral infections.

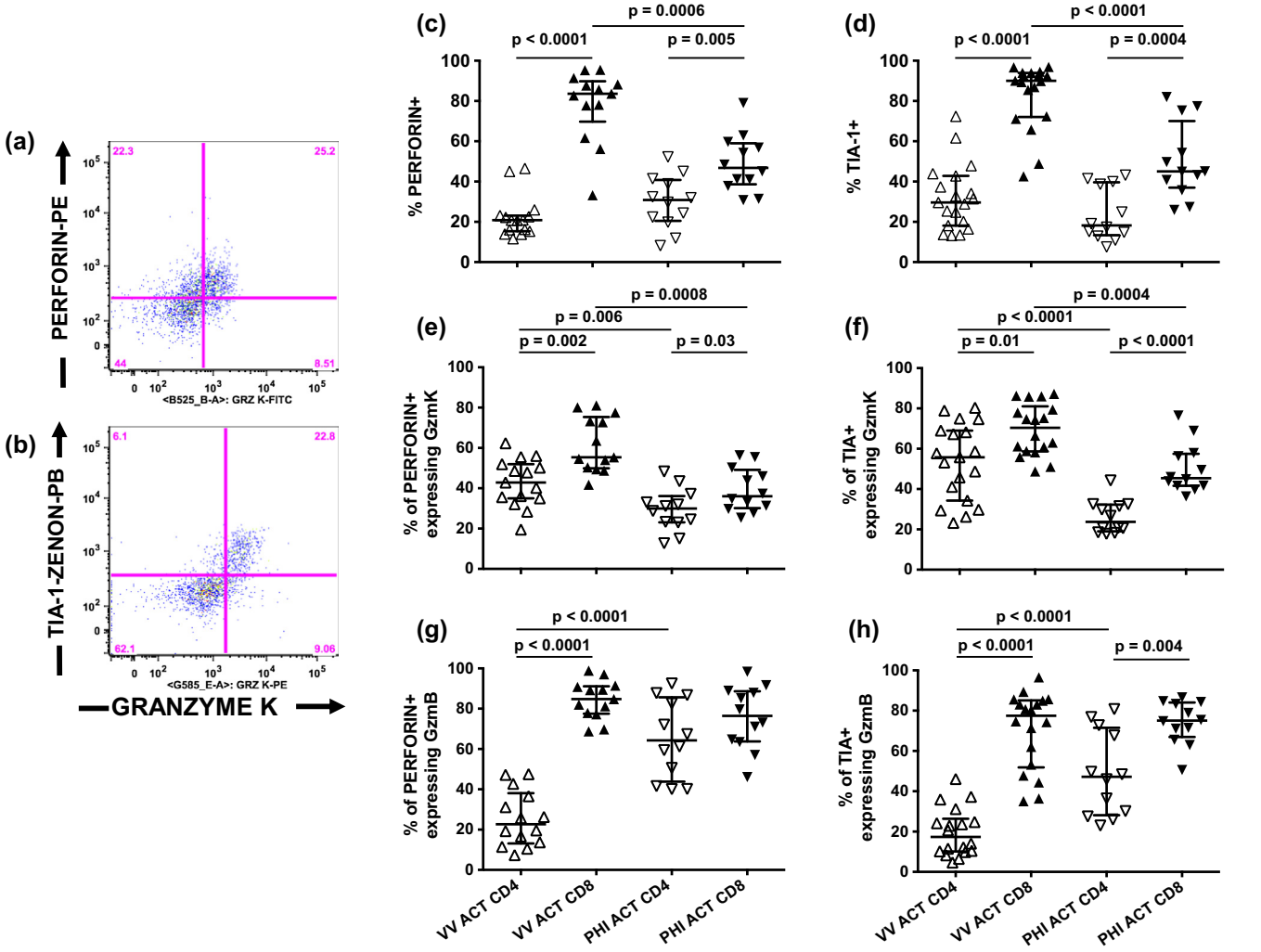

Fig. 4. Comparison of perforin and TIA-1 expression in activated CD4 and CD8 T-cells following vaccination with *Vaccina virus* and during PHI. Representative flow plots of the CD3+CD4+ co-expression of (a) perforin and granzyme K and (b) TIA-1 and granzyme K. Phenotypic analysis of CTL markers (c) perforin and (d) TIA-1 of both CD4 and CD8 T-cells in response to VV (n = 13–19) and PHI (n = 12). Proportion of CD4 and CD8 T-cells that are perforin+ and expressing (e) GzmK (VV: n = 13–15; PHI: n = 12) and (g) GzmB (VV: n = 14; PHI: n = 12). Proportion of CD4 and CD8 T-cells that are TIA-1+ and expressing (f) GzmK (VV: n = 18–19; PHI: n = 12) and (h) GzmB (VV: n = 18; PHI: n = 12). Medians and interquartile ranges are shown.

No difference in expression of perforin (Fig. 4a) or TIA-1 (Fig. 4b) was found between activated CD4 T-cells from VV or PHI (Fig. 4c and d). Perforin (Fig. 4c) and TIA-1 (Fig. 4d) expression was significantly higher in CD8 compared to CD4 T-cells from either VV (perforin median: CD8: 84%, CD4: 21%; TIA-1 median: CD8: 90%; CD4: 30%) or PHI subjects (perforin median: CD8: 47%, CD4: 31%; TIA-1 median: CD8: 45%; CD4: 18%). Interestingly, activated CD8 T-cells in response to VV had significantly higher expression of both perforin (Fig. 4c) and TIA-1 (Fig. 4d) than in response to PHI.

Analysis of GzmK expression within these subsets showed that primary CD4 and CD8 T-cell responses to VV involves a greater proportion of cells expressing this molecule than in PHI (Fig. 4e and f). In response to VV, a median 43% of perforin+activated CD4 T-cells expressed GzmK compared to 30% of these cells in response to PHI (Fig. 4e). For CD8+perforin+T-cells a median 55% expressed GzmK in response to VV compared to a median 36% in response to PHI (Fig. 4e). A higher percentage of TIA-1+ CD4 T-cells expressed GzmK (median: 57%) in response to VV than in response to PHI (median: 24%, Fig. 4f). The same was true for TIA-1+ CD8 T-cells, with a median 70% expressing GzmK in response to VV compared to 45% in response to PHI (Fig. 4f).

GzmB was more highly expressed in CD4 T-cells responding to PHI, a median 64% of CD4+perforin+ T-cells expressed GzmB compared to VV (median: 23%, Fig. 4g). A higher proportion of CD4 TIA-1+ cells expressed GzmB in response to PHI (median: 47%) compared to VV (median: 17%, Fig. 4h). No difference in expression of GzmB within CD8 T-cells expressing perforin or TIA-1 was seen between the response to VV and PHI.

3.6. Phenotype of activated CD4 T-cells at Day-13 post-VV vaccination vs PHI

Despite similar levels of CD4 T-cell activation in response to VV and PHI, significant phenotypic differences were observed. VV-activated CD4 T-cells had higher co-expression of CCR5 and CD127 (median: 35%) compared to activated CD4 T-cells measured during PHI (median: 12%, Fig. 5a and c). Indicating the VV CD4 T-cells are likely more long-lived than those in response to PHI.

Of the activated CD4 T-cells that were CCR5+CD127+ a differential pattern of homing receptor expression was observed in response to the two viruses. The VV response revealed the CCR5 +CD127+ activated CD4 T-cells were more likely homing to lymph nodes as they had significantly higher expression of CD62L

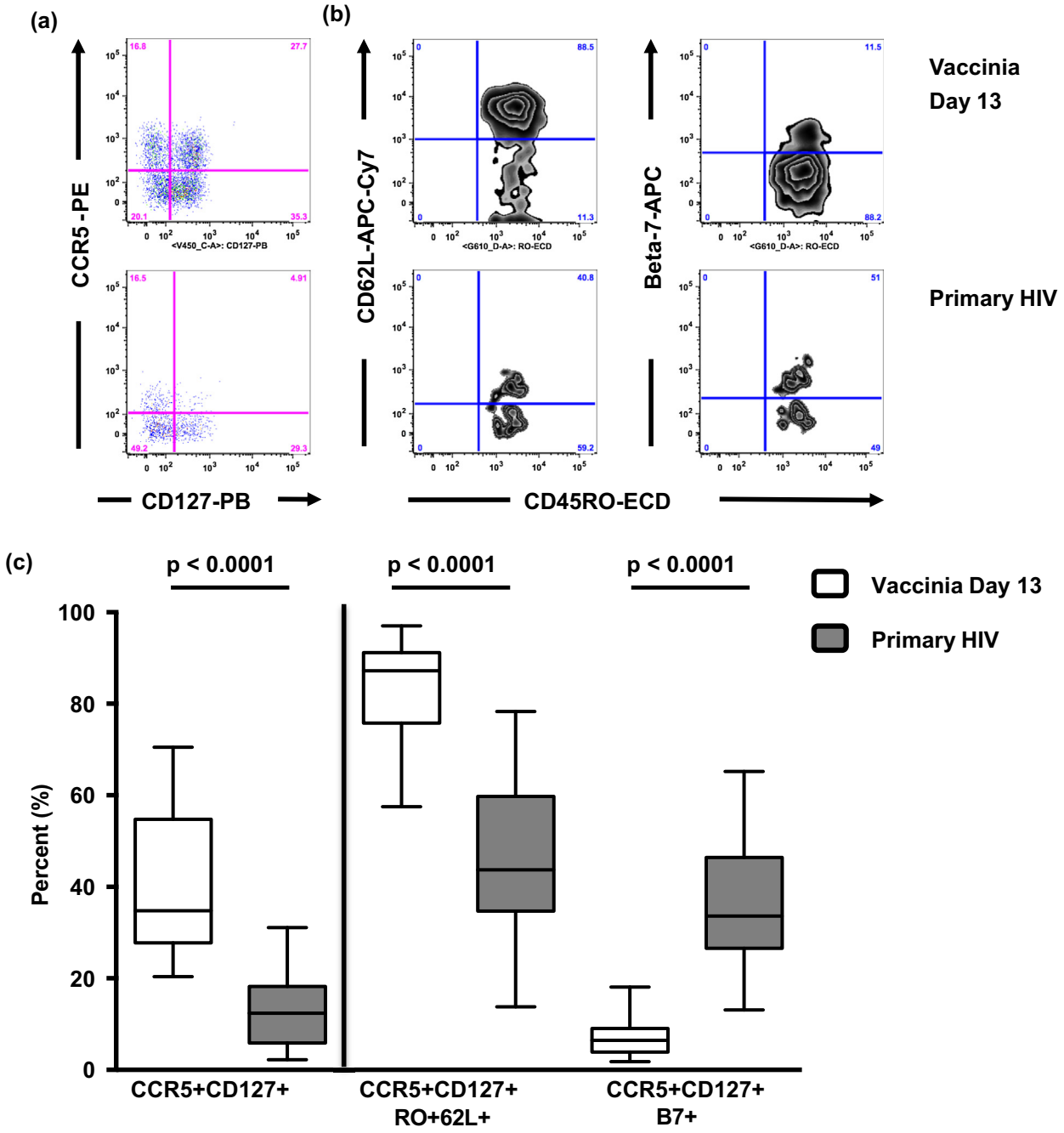

Fig. 5. Immunophenotyping of activated CD4 T-cells in response to VV (n = 19) and HIV-1 (n = 12). Representative flow plots of (a) CCR5 and CD127 co-expression on CD3+CD4+CD38+CD45RO+ T-cells and (b) expression of CD62L and integrin β7 on the CCR5+CD127+ activated CD4 T-cells. (c) Differential co-expression of CCR5 and CD127, the right-hand side of the graph shows the % of CCR5+CD127+CD4 T-cells that are CD45RO+CD62L+ and express the gut-homing receptor, integrin β7. The box-and-whisker plots represent the minimum, 25th percentile, median, 75th percentile and maximum values.

(median: 87%) compared to PHI (median: 44%, Fig. 5b and c). In response to PHI, activated CCR5+CD127+ CD4 T-cells were more likely homing to gut-associated lymphoid tissue as they had significantly higher expression of the gut-homing receptor integrin β7 (median: 33.6%) compared to VV (median: 6.5%, Fig. 5b and c).

3.7. VV-specific T-cell lines generated from day-13 and 12 months post-vaccination display functional cytotoxic activity

Using mass spectrometry two HLA-DR restricted VV-epitopes, DPD (DPDHYKDYAFIQWTGGNIRN) and DPL (DPLYIYKMFQNAKIDVD) were identified. VV-specific T-cell lines generated to DPD and DPL were tested for cytotoxicity potential (CD107a degranulation assay, Fig. 6a; and LDH-release, Fig. 6b). DPD and DPL CD4 T-cell lines displayed 62% and 30% cytotoxicity respectively at a 25:1 effector to target ratio with the LDH-release assay (Fig. 6b). The same effector to target ratio for HLA-mismatched controls showed 4% and 16% cytotoxicity (Fig. 6b).

Utilizing the CD107a assay, VV-specific T-cell lines generated from PBMC at day-13 (DPL) and 12 months post-vaccination (DPD and DPL) exhibit degranulation (Fig. 6a and c) when challenged with HLA-matched peptide loaded APC. At 25:1 effector to APC ratio, there was 5% co-expression of CD69 with CD107a for the day-13 DPL cell line and 29.7% co-expression for the 12 month DPL

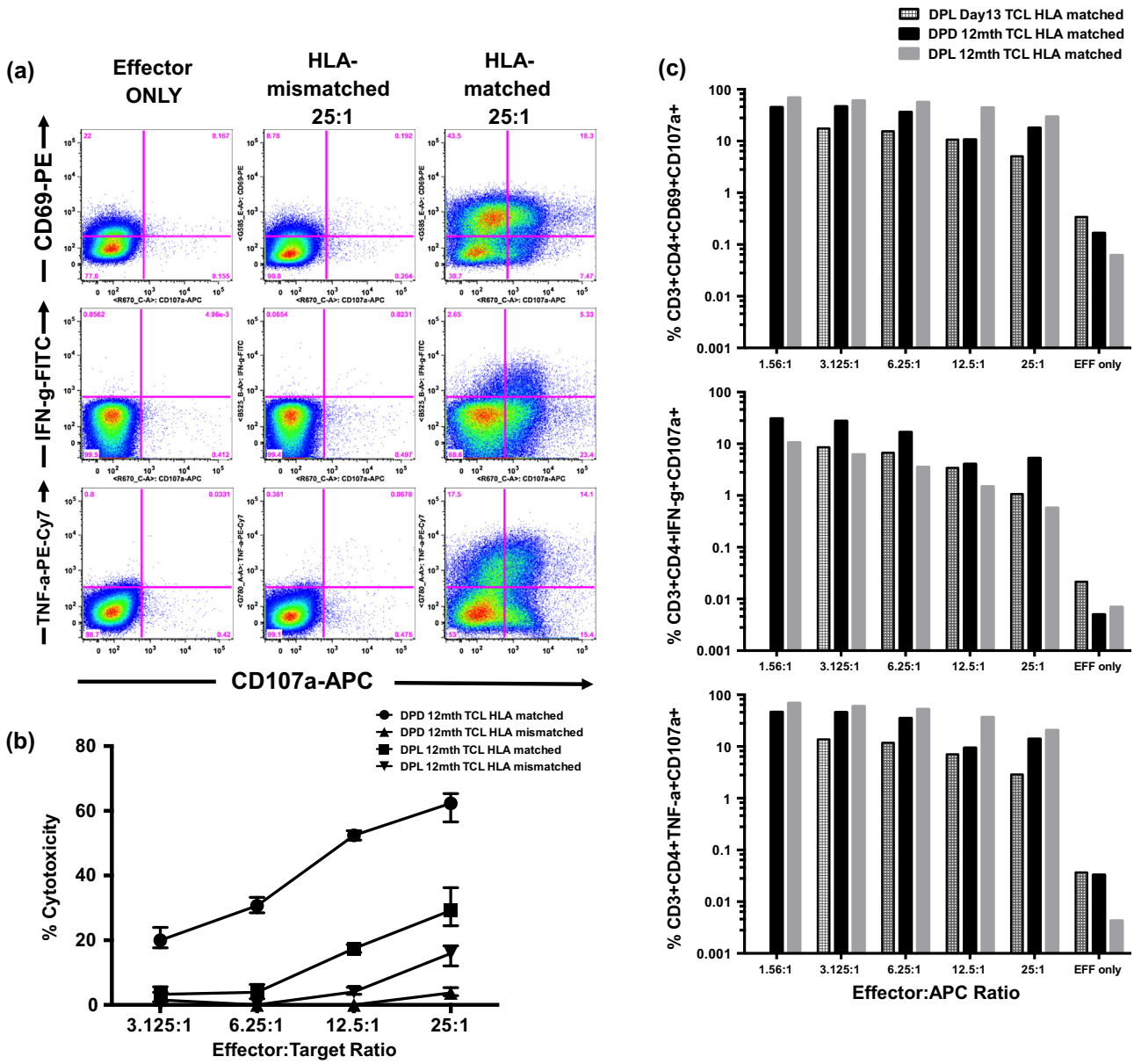

Fig. 6. VV-specific T-cell lines display functional cytotoxic activity. (a) Representative flow plots of CD3+CD4+ T-cell lines, showing co-expression of CD69, IFN-γ and TNF-α with CD107a (top to bottom) and effector only, HLA-mismatched and HLA-matched at 25:1 effector to APC ratio (left to right). (b) VV-specific CD4 T-cell lines from 12 months post vaccination expanded to DPD and DPL VV peptides show cytotoxicity using the LDH assay at varying effector to target ratios in triplicate. Error bars show mean with range. (c) Percentage of VV-specific CD3+CD4+ T-cell lines from 13-days post-vaccination (DPL) and 12 months-post vaccination (DPD and DPL) that are CD69+CD107a+ (top) IFN-γ+CD107a+ (middle) and TNF-α+ CD107a+ (bottom). HLA-mismatched values have been subtracted from HLA-matched values.

cell line (Fig. 6c). Co-expression of IFN-γ and TNF-α with CD107a was detected for all VV-specific cell lines (Fig. 6c). Therefore, cytotoxic potential for T-cell lines against autologous VV-epitopes during both acute and memory phases of VV-inoculation was demonstrated.

4. Discussion

CD4 T-cells with cytotoxic characteristics have been described in the literature over the past 30 years. Some of the first reports were from cultured CD4 T-cell lines and clones isolated from humans and mice [29,30]. Initially there was uncertainty as to whether these CD4 T-cells were true CTLs or an anomaly due to long-term *in vitro* cultures [31], increasing reports are however demonstrating cytolytic CD4 T-cell responses are an important anti-viral cell subset *in vivo* [1–8].

Cytotoxic CD4 T-cells utilise two main cytotoxic effector mechanisms also utilised by CD8 CTLs and natural killer cells (NKs). The Fas/Fas ligand-mediated pathway [32] and directed exocytosis of cytotoxic granules into target cells to induce apoptosis (reviewed in [33]). Cytotoxic granules that contain perforin, granzymes and granulysin are specialised storage granules that undergo exocytosis after specific TCR signalling. The pore forming protein, perforin, enables direct transfer of cytotoxic molecules such as granzymes into target cells. In humans, there are five known granzymes (A, B, H, K and M) with various substrate specificities (reviewed in [34–37]).

Our study of the gene expression profile and immuno-phenotyping of CD45RO+CD38++ CD4 T-cells at day-13 post-VV-vaccination suggests that CD4 T-cells with cytotoxic properties are expanded in the early primary immune response to VV. In parallel to these observations, we demonstrate VV-specific

CD4 T-cell lines up-regulate the machinery of cytotoxic degranulation and subsequently lyse HLA-matched target cells, loaded with autologous VV-peptides. Moreover, this CTL activity is carried from acute VV replication (day-13) into the quiescent memory T-cell phase.

We show activated CD4 T-cells express high levels of GzmK 13-days post-VV-vaccination. GzmK has previously been reported to play a role in CD8 T-cell responses to viral infections including Flu, CMV, EBV, HIV and dengue fever [38–40]. In our study, CD4 and CD8 T-cells expressing perforin or TIA-1 in response to VV were shown to have higher co-expression of GzmK than those cells responding to PHI. In contrast, GzmB was more highly expressed in CD4 T-cells responding to PHI. The divergent expression of GzmB and GzmK in response to these two viral infections may be due to the time point these cells were measured post infection (VV: day-13; PHI: median 25-days) or the differentiation stage of these cells as has been previously reported for CD8 T-cells [38,40].

We speculate that activated CD4 T-cells in response to VV *in vivo* could use these CTL molecules in a coordinated fashion to trigger apoptosis in target cells that express major histocompatibility complex class II molecules for recognition. Likely targets are antigen-presenting cells such as dendritic cells, monocytes, macrophages and B cells or even other CD4 cells. It is plausible that GzmK expressing activated CD4 T-cells play a role in immune regulation and perhaps represent another form of regulatory T-cells.

Cytotoxic markers such as those discussed here have been extensively studied in CD8 CTL and NKs (reviewed in [41]). Importantly, these markers of cytotoxicity are clearly associated in murine models of viral infection with transient activated effector phenotype CD8 T-cells that eventually become long-term memory cells [42,43]. It is plausible these markers are similarly expressed in the differentiation pathway of human anti-viral memory CD4 T-cells.

This is the first description of CD4 CTL playing a role in the primary immune response to VV. The data presented suggests that CD4 T-cells expressing CTL molecules may be important in determining the nature and effectiveness of the eventual immune response. Understanding the role of this distinct CD4 T-cell subset in the generation of effective memory may lead us closer to the development of more effective vaccines for diseases such as HIV.

Conflict of interest

The authors declare no conflict of interest.

Acknowledgements

Members of the PHIIDO study group are: Robert McFarlane, David Baker, Marilyn McMurchie at East Sydney Doctors, Mark Boyd, Andrew Carr, Anthony Kelleher at St Vincent's Hospital Sydney, Mark Bloch at Holdsworth House Medical Practice, Robert Finalyson at Taylor Square Private Clinic, Derek Chan at Albion Street Clinic, and Pat Grey, Ansari Shaik The Kirby Institute, UNSW Australia, Sydney, New South Wales, Australia.

The authors would like to thank the VV vaccine volunteers who participated in this study, the PHIIDO patients, the clinical trials team at St Vincent's Centre for Applied Medical Research, Bertha Fsadni, Maria Piperias, Julie Yeung and Kate Merlin for PBMC processing and storage, Ken Field for help with cell sorting, Trina So for help with microarrays, Wayne Dyer for vaccinia viral lysate, Charani Ranasinghe and Tamara Cooper for help with subject recruitment and Thakshila Amarasena for help with blood collection.

This work was supported by grants from the Australian National Health and Medical Research Council (351041 to CMLM, 510448 to DAC, SJK and ADK, 1052979 to DAC, SJK and ADK).

Appendix A. Supplementary material

Supplementary data associated with this article can be found, in the online version, at http://dx.doi.org/10.1016/j.vaccine.2016.09.009.

References

[1] Appay V, Zaunders JJ, Papagno L, Sutton J, Jaramillo A, Waters A, et al. Characterization of CD4(+) CTLs ex vivo. J Immunol 2002;168:5954–8.
[2] Zaunders JJ, Dyer WB, Wang B, Munier ML, Miranda-Saksena M, Newton R, et al. Identification of circulating antigen-specific CD4+ T lymphocytes with a CCR5+, cytotoxic phenotype in an HIV-1 long-term nonprogressor and in CMV infection. Blood 2004;103:2238–47.
[3] Soghoian D, Jessen H, Flanders M, Sierra-Davidson K, Cutler S, Pertel T, et al. HIV-specific cytolytic CD4 T cell responses during acute HIV infection predict disease outcome. Sci Transl Med 2012;4. 123ra25.
[4] Johnson S, Eller M, Teigler JE, Maloveste SM, Schultz BT, Soghoian DZ, et al. Cooperativity of HIV-specific cytolytic CD4 T cells and CD8 T cells in control of HIV viremia. J Virol 2015;89:7494–505.
[5] Suni M, Ghanekar S, Houck D, Maecker H, Wormsley S, Picker L, et al. CD4(+) CD8(dim) T lymphocytes exhibit enhanced cytokine expression, proliferation and cytotoxic activity in response to HCMV and HIV-1 antigens. Eur J Immunol 2001;31:2512–20.
[6] van Leeuwen E, Remmerswaal E, Vossen M, Rowshani A, Wertheim-van Dillen P, van Lier R, et al. Emergence of a CD4+CD28-granzyme B+, cytomegalovirus-specific T cell subset after recovery of primary cytomegalovirus infection. J Immunol 2004;173:1834–41.
[7] Omiya R, Buteau C, Kobayashi H, Paya C, Celis E. Inhibition of EBV-induced lymphoproliferation by CD4(+) T cells specific for an MHC class II promiscuous epitope. J Immunol 2002;169:2172–9.
[8] Aslan N, Yurdaydin C, Wiegand J, Greten T, Ciner A, Meyer M, et al. Cytotoxic CD4 T cells in viral hepatitis. J Viral Hepat 2006;13:505–14.
[9] Wahid R, Cannon M, Chow M. Virus-specific CD4+ and CD8+ cytotoxic T-cell responses and long-term T-cell memory in individuals vaccinated against polio. J Virol 2005;79:5988–95.
[10] de Souza M, Ratto-Kim S, Chuenarom W, Schuetz A, Chantakulkij S, Nuntapinit B, et al. The Thai phase III trial (RV144) vaccine regimen induces T cell responses that preferentially target epitopes within the V2 region of HIV-1 envelope. J Immunol 2012;188:5166–76.
[11] Sacha J, Giraldo-Vela J, Buechler M, Martins M, Maness N, Chung C, et al. Gag- and Nef-specific CD4+ T cells recognize and inhibit SIV replication in infected macrophages early after infection. Proc Natl Acad Sci USA 2009;106:9791–6.
[12] Demkowicz WJ, Littaua R, Wang J, Ennis F. Human cytotoxic T-cell memory: long-lived responses to *Vaccinia virus*. J Virol 1996;70:2627–31.
[13] Zaunders JJ, Dyer WB, Munier ML, Ip S, Liu J, Amyes E, et al. CD127+CCR5+CD38+++ CD4+ Th1 effector cells are an early component of the primary immune response to *Vaccinia virus* and precede development of interleukin-2+ memory CD4+ T cells. J Virol 2006;80:10151–61.
[14] Zaunders JJ, Ip S, Munier ML, Kaufmann DE, Suzuki K, Brereton C, et al. Infection of CD127+ (interleukin-7 receptor+) CD4+ cells and overexpression of CTLA-4 are linked to loss of antigen-specific CD4 T cells during primary human immunodeficiency virus type 1 infection. J Virol 2006;80:10162–72.
[15] Munier C, Zaunders J, Ip S, Cooper D, Kelleher A. A culture amplified multi-parametric intracellular cytokine assay (CAMP-ICC) for enhanced detection of antigen specific T-cell responses. J Immunol Methods 2009;345:1–16.
[16] Zaunders J, Munier M, Seddiki N, Pett S, Ip S, Bailey M, et al. High levels of human antigen-specific CD4+ T cells in peripheral blood revealed by stimulated coexpression of CD25 and CD134 (OX40). J Immunol 2009;183:2827–36.
[17] Baugh L, Hill A, Brown E, Hunter C. Quantitative analysis of mRNA amplification by in vitro transcription. Nucleic Acids Res 2001;29:E29.
[18] Reich M, Liefeld T, Gould J, Lerner J, Tamayo P, Mesirov JP. GenePattern 2.0. Nat Genet 2006;38:500–1.
[19] Wettenhall JM, Smyth GK. LimmaGUI: a graphical user interface for linear modeling of microarray data. Bioinformatics 2004;20:3705–6.
[20] Suzuki K, Shijuuku T, Fukamachi T, Zaunders J, Guillemin G, Cooper D, et al. Prolonged transcriptional silencing and CpG methylation induced by siRNAs targeted to the HIV-1 promoter region. J RNAi Gene Silencing 2005;1:66–78.
[21] Dudek NL, Croft NP, Schittenhelm RB, Ramarathinam SH, Purcell AW. A systems approach to understand antigen presentation and the immune response. Methods Mol Biol 2016;1394:189–209.
[22] Croft NP, Smith SA, Wong YC, Tan CT, Dudek NL, Flesch IE, et al. Kinetics of antigen expression and epitope presentation during virus infection. PLoS Pathog 2013;9:e1003129.
[23] Shilov IV, Seymour SL, Patel AA, Loboda A, Tang WH, Keating SP, et al. The paragon algorithm, a next generation search engine that uses sequence temperature values and feature probabilities to identify peptides from tandem mass spectra. Mol Cell Proteomics 2007;6:1638–55.
[24] Illing PT, Vivian JP, Dudek NL, Kostenko L, Chen Z, Bharadwaj M, et al. Immune self-reactivity triggered by drug-modified HLA-peptide repertoire. Nature 2012;486:554–8.

[25] Yssel H, Spits H. Generation and maintenance of cloned human T cell lines. Curr Protoc Immunol 2002. Chapter 7: Unit 7 19.
[26] Betts MR, Koup RA. Detection of T-cell degranulation: CD107a and b. Methods Cell Biol 2004;75:497–512.
[27] Sallusto F, Lenig D, Mackay CR, Lanzavecchia A. Flexible programs of chemokine receptor expression on human polarized T helper 1 and 2 lymphocytes. J Exp Med 1998;187:875–83.
[28] Bonecchi R, Bianchi G, Bordignon PP, D'Ambrosio D, Lang R, Borsatti A, et al. Differential expression of chemokine receptors and chemotactic responsiveness of type 1 T helper cells (Th1s) and Th2s. J Exp Med 1998;187:129–34.
[29] Billings P, Burakoff S, Dorf M, Benacerraf B. Cytotoxic T lymphocytes specific for I region determinants do not require interactions with H-2K or D gene products. J Exp Med 1977;145:1387–92.
[30] Maimone M, Morrison L, Braciale V, Braciale T. Features of target cell lysis by class I and class II MHC-restricted cytolytic T lymphocytes. J Immunol 1986;137:3639–43.
[31] Fleischer B. Acquisition of specific cytotoxic activity by human T4+ T lymphocytes in culture. Nature 1984;308:365–7.
[32] Kischkel F, Hellbardt S, Behrmann I, Germer M, Pawlita M, Krammer P, et al. Cytotoxicity-dependent APO-1 (Fas/CD95)-associated proteins form a death-inducing signaling complex (DISC) with the receptor. EMBO J 1995;14:5579–88.
[33] Trapani J, Smyth M. Functional significance of the perforin/granzyme cell death pathway. Nat Rev Immunol 2002;2:735–47.
[34] Chowdhury D, Lieberman J. Death by a thousand cuts: granzyme pathways of programmed cell death. Annu Rev Immunol 2008;26:389–420.
[35] Cullen S, Brunet M, Martin S. Granzymes in cancer and immunity. Cell Death Differ 2010;17:616–23.
[36] Anthony D, Andrews D, Watt S, Trapani J, Smyth M. Functional dissection of the granzyme family: cell death and inflammation. Immunol Rev 2010;235:73–92.
[37] Bovenschen N, Kummer J. Orphan granzymes find a home. Immunol Rev 2010;235:117–27.
[38] Harari A, Enders F, Cellerai C, Bart P, Pantaleo G. Distinct profiles of cytotoxic granules in memory CD8 T cells correlate with function, differentiation stage, and antigen exposure. J Virol 2009;83:2862–71.
[39] Hertoghs K, Moerland P, van Stijn A, Remmerswaal E, Yong S, van de Berg P, et al. Molecular profiling of cytomegalovirus-induced human CD8+ T cell differentiation. J Clin Invest 2010;120:4077–90.
[40] Bratke K, Kuepper M, Bade B, Virchow JJ, Luttmann W. Differential expression of human granzymes A, B, and K in natural killer cells and during CD8+ T cell differentiation in peripheral blood. Eur J Immunol 2005;35:2608–16.
[41] Barry M, Bleackley R. Cytotoxic T lymphocytes: all roads lead to death. Nat Rev Immunol 2002;2:401–9.
[42] Opferman J, Ober B, Ashton-Rickardt P. Linear differentiation of cytotoxic effectors into memory T lymphocytes. Science 1999;283:1745–8.
[43] Jacob J, Baltimore D. Modelling T-cell memory by genetic marking of memory T cells in vivo. Nature 1999;399:593–7.